Dimers and divacancy effects on a reconstructed Si(001) surface

H. S. Lim, K. C. Low, and C. K. Ong
Department of Physics, National University of Singapore, Kent Ridge, Singapore 0511
(Received 7 December 1992; revised manuscript received 17 February 1993)

We have employed a tight-binding molecular-dynamics scheme to study the structural and dynamical behavior of dimers and the divacancy on a Si(001) surface at room temperature. At $T=0$ K, we conclude that dimers are intrinsically asymmetric but they fluctuate to give on a time average a symmetric appearance at room temperature. However, the presence of a divacancy defect is found to induce and stabilize the formation of buckled dimers in its vicinity. These dimers, in addition, are found to be twisted although, in the defect-free surface, none appears so. A detailed analysis of the structural and dynamical properties of the defect and its influence on the behavior of neighboring dimers is presented and discussed.

I. INTRODUCTION

Si(001) surface reconstructions have been studied intensively both theoretically[1-5] and experimentally[6-9] over the past decades. The majority of evidence currently points to a model where the outermost Si atoms form dimers,[2] whereby the number of dangling bonds is substantially reduced. However, the nature of these dimers—whether they are buckled (asymmetric model) or not (symmetric model)—is still being discussed. It is an important question since the surface charge density and the gap of the electronic surface states depend rather strongly on the magnitudes of dimer buckling. In a recent scanning-tunneling microscopy (STM) experiment, Tromp, Hamers, and Demuth[6] studied the Si(001) surface with extremely high lateral resolution and observed the coexistence of buckled and unbuckled dimers in roughly equal amounts at room temperature. In particular, they have observed the formation of buckled dimer domains only near vacancies and step edges. However, remote dimers under the weak influence of such defects appear as symmetric.

In a recent paper, Weakliem, Smith, and Carter[11] investigated the dynamic structure of a defect-free reconstructed Si(001) surface using Stillinger-Weber classical potentials. They found that the surface does not just consist of only symmetric or only buckled dimers but rather a rapidly interconverting mixture of the two such that, on a time average, only symmetric dimers are observed. However, similar studies involving the presence of defects have not been done and such works must clearly entail quantum-mechanical descriptions to be accurate and reliable. This is because classical calculations can neither account for electronic relaxation effects nor describe purely quantum-mechanical phenomena such as Jahn-Teller distortions and charge transfer among atoms.

In this paper, we employ a semiempirical tight-binding molecular-dynamics (TBMD) (Ref. 12) scheme to study the Si(001) surface. This scheme was found to be computationally efficient; moreover, it affords an accurate treatment of fairly large and complex Si systems for a reasonably long period of time. Our goals are to describe and characterize in detail the structural properties of a divacancy defect and to investigate, in particular, the room-temperature behavior of dimers under the influence of this defect. At room temperature, our simulations indicate the coexistence of $p(2\times2)$- and $c(2\times4)$-like reconstructions. The dimers are observed to oscillate but, on the time average over 4000 time steps (≈0.44 ps), they are buckled and no symmetric dimers are present near the defect. This provides theoretical support for the earlier speculations[6,10] that defects induce and stabilize dimer bucklings but have hitherto not been shown. In addition, since what has been observed in STM is usually complicated by the possibilities of impurity contamination and the actual structure of a divacancy, and its influence is therefore largely unknown, we provide, for the first time to our knowledge, a detailed structural analysis of this defect on a Si(001) surface. We find that this particular defect has an asymmetric appearance that not only induces buckling but also slight twisting in neighboring dimers. Its structural properties are found to be similar to those observed in STM.[10,6]

II. COMPUTATIONAL DETAILS

A. Total energy for Si(001) slab

We employ the TBMD scheme of Khan and Broughton[12] and adopt their various tight-binding parameter values. The total-energy expression due to Tománek and Schlüter[13] had been modified by Khan and Broughton[12] to include a smooth cutoff function so as to permit molecular-dynamics simulations. We also follow their scheme of constructing a fictitious Lagrangian to simulate the physical trajectories of the nuclei while keeping the electrons close to their quantum ground state.

Consider a slab of five layers of Si atoms with $N/5$ (i.e., 32) atoms per layer for a total of $N=160$ atoms. The top layer in the positive z direction forms the surface, for which we study surface reconstructions and the divacancy effects. Periodic boundary conditions are applied in the plane of the surface to simulate a surface extending to

infinity in the x and y directions. The dangling bonds of the Si atoms at the bottom layer are saturated by N_H hydrogenlike atoms that are used to mimic closely the bulk Si atoms.

In our simulations, the ions in the top four layers are allowed to move and interact with neighboring atoms while the last two bottom layers (Si and the N_H hydrogen atoms in the fifth and sixth layers, respectively) are kept fixed but are allowed to change their electronic structures as a result of interaction with neighboring atoms. Each silicon and hydrogen atom contributes four electrons and one electron, respectively, giving a total of $4N+N_H$ electrons. Since our problem is nonmagnetic, there are $2N+N_H/2$ independent states $\{\Phi_i\}$, each being occupied by two (spin-up and spin-down) electrons. These states are expanded in terms of a basis set $\{\phi_{l\alpha},\phi_l^H\}$ consisting of $(4N+N_H)$ elements, where $\phi_{l\alpha}$ denotes a particular orbital (s, p_x, p_y, or p_z orbital corresponding to $\alpha=1$, 2, 3, or 4) located on the lth Si atom and ϕ_l^H is an s orbital located on the lth hydrogen atom:

$$\Psi_i(\mathbf{r})=\sum_{l=1}^{N}\sum_{\alpha=1}^{4}c_{l\alpha}^i\phi_{l\alpha}(\mathbf{r})+\sum_{l=1}^{N_H}c_l^{Hi}\phi_l^H(\mathbf{r}) , \tag{1}$$

where $i=1,2,\ldots,2N+N_H/2$.

The total energy $E^{\rm tot}$ of this slab is given by

$$E^{\rm tot}=E^{\rm BS}+E_2-E_3+E_4 , \tag{2}$$

where

$$E^{\rm BS}=2\sum_{i}^{2N+N_H/2}\langle\Phi_i|H|\Phi_i\rangle-NE_{\rm Si}^0-N_HE_H^0 , \tag{3}$$

$$E_2=\sum_{l=2}^{N}\sum_{l'=1}^{l-1}E_r(|\mathbf{R}_l-\mathbf{R}_{l'}|) , \tag{4}$$

$$E_3=N\left[\phi_1\left[\frac{n_b}{N}\right]^2+\phi_2\left[\frac{n_b}{N}\right]+\phi_3\right] , \tag{5}$$

$$E_4=U\sum_{l=1}^{N}(q_l-q_l^0)^2+U_H\sum_{l=1}^{N_H}(q_l^{\rm H}-q_l^{0H})^2 . \tag{6}$$

where $E^{\rm BS}$ is the electronic band-structure term, E_2 is the repulsive term which contains ion-ion interactions and exchange-correlation energies as well as accounting for the double counting of electron-electron interactions in $E^{\rm BS}$, E_3 is the term that prevents the system from always favoring metallic close-packed structure, and E_4 is the "Hubbard-like" term that prevents the system from having large charge transfer among atoms.[13] Note that E_H^0 is the energy of the isolated "hydrogen" atom.

The repulsive term E_2 is slightly different from that used by Khan and Broughton [Eq. (14) of Ref. 12)] in that the additional contribution from the "hydrogen" atoms is here set to zero since the fifth Si layer in our sample is kept fixed throughout the simulations.

Finally, the charges on the silicon and "hydrogen" atoms q_l and q_l^H are given by

$$q_l=2\sum_{i=1}^{2N+N_H/2}\sum_{\alpha=1}^{4}(c_{l\alpha}^i)^2,\quad q_l^0=4.0 , \tag{7}$$

$$q_l^H=2\sum_{i=1}^{2N+N_H/2}(c_l^{Hi})^2,\quad q_l^{0H}=1.0 . \tag{8}$$

B. Molecular dynamics for the electrons and ions

We use molecular dynamics to simulate both the ionic and electronic trajectories where the forces are calculated by a "fictitious Lagrangian" method.[12] To reduce the number of indices, we combine the coefficients of expansions of the occupied wave functions i [Eq. (1)] into a single vector of dimensionality $N_T\equiv4N+N_H$ with elements c_m^i, whose first $4N$ elements are defined by $c_{4(l-1)+\alpha}^i=c_{l\alpha}^i$, and the last N_H elements by $c_{4N+l}^i=c_l^{Hi}$. The classical Lagrangian L is given by

$$L=\tfrac{1}{2}\mu\sum_{i,m}(\dot c_m^i)^2+\tfrac{1}{2}M\sum_l\dot{\mathbf{R}}_l^2-E^{\rm tot}[\{\mathbf{R}_l\},\{c_m^i\}] , \tag{9}$$

while the orthonormality of the occupied states requires the following constraining equations:

$$\sum_{m=1}^{N_T}c_m^ic_m^j-\delta_{ij}=0 . \tag{10}$$

These lead to the following equations of motion for the ionic and electronic coordinates:

$$M\ddot{\mathbf{R}}_l=-\frac{\partial}{\partial\mathbf{R}_l}E^{\rm tot}[\{\mathbf{R}_l\},\{c_m^i\}] \tag{11}$$

and

$$\mu\ddot c_m^i=-\frac{\partial}{\partial c_m^i}E^{\rm tot}[\{\mathbf{R}_l\},\{c_m^i\}]+\sum_j\Lambda_{ij}c_m^j . \tag{12}$$

Here i and j run over the occupied states 1, 2, ..., $N_T/2$, and Λ_{ij} is a symmetric matrix whose elements are the Lagrange multipliers[12] given by

$$\Lambda_{ij}=\sum_{m=1}^{N_T}\left[\frac{1}{2}\frac{\partial E^{\rm tot}}{\partial c_m^i}c_m^j+\frac{1}{2}\frac{\partial E^{\rm tot}}{\partial c_m^j}c_m^i-\mu\dot c_m^i\dot c_m^j\right] . \tag{13}$$

The simulation of the ionic dynamics proceeds as follows. For a given position of the ions, the electrons are quenched to the Born-Oppenheimer (BO) surface by a self-consistent diagonalization of an $N_T\times N_T$ Hamiltonian matrix. After each quench, both the trajectories of the ionic and electronic coordinates are updated simultaneously by integrating equations (11) and (12) with the Verlet algorithm. This is repeated for $N_{\rm Born}$ (=100 in this work) time steps, after which the electrons are quenched to the BO surface again and the procedure repeated. During the $N_{\rm Born}$ steps, a "Shake" algorithm[14] is used to impose the orthonormality constraints of Eq. (10) in the updating of the electronic coordinates $\{c_m^j\}$.

Our first aim is to determine the possible global minimum for the Si(001) surface structure. We start with a reconstructed Si(001)-2×1 surface consisting of only symmetric dimers with arbitrary dimer bond lengths. The system is heated up and then cooled slowly to $T=0$ K by appropriately scaling the velocities of the atoms. This annealing treatment is repeated for a few more initial arbitrary dimer configurations so that the likelihood

of obtaining the optimum structural configuration is higher.

To study the room-temperature behavior of dimers in the vicinity of a divacancy, a dimer is initially removed from a reconstructed Si(001)-2×1 unbuckled surface. The system is heated and equilibrated at $T=300$ K and for the next 4000 time steps (one step corresponding to 0.11×10^{-15} s), the dimer tilt Δz in the z direction normal to the surface is computed for each dimer where $\Delta z_{ij}=z_i-z_j$, z_i and z_j being the z coordinates of atom i and atom j, respectively. We have also looked for possible dynamic y twisting of the dimers, given that the dimer row is in the y direction (i.e., $\langle\bar{1}10\rangle$), by similarly calculating Δy as a function of time for each dimer. Lastly, we use the notation dimer(i,j) to denote a dimer formed from atom i and atom j.

III. RESULTS AND DISCUSSIONS

The optimum structural configuration is shown in Fig. 1. It has $c(4\times2)$ symmetry, but we have also observed among the annealed samples structures having similar energies to this optimum configuration and exhibiting phase-coexistence regions of local $p(2\times2)$ and $c(4\times2)$ symmetries. However, since energies calculated with TB models are usually unreliable when energy differences are small, we could only conclude that these $p(2\times2)$ and $c(4\times2)$ structures have essentially the same energy. For instance, if we define ΔE^s as the $p(2\times2)$ reconstruction surface energy per unit surface atom with respect to the ground-state $c(4\times2)$ reconstruction, i.e.,

$$\Delta E^s=\frac{E^{\rm tot}[p(2\times2)]-E^{\rm tot}[c(4\times2)]}{N_S}\ , \tag{14}$$

where N_S is the number of surface atoms ($N_S=32$ in this work), ΔE^s is calculated to be 5.8 (meV/surface atom).

What is important, however, is that all the annealed samples consist of buckled dimers only. The result suggests that dimers are intrinsically asymmetric. As we have started off with initially symmetric dimers, clearly the number of buckled dimers must have grown at the expense of the symmetric dimers, in agreement with recent STM observations.[10] Wolkow has observed that on cooling the Si(100) to 120 K, the number of buckled dimers on this surface increases. It should be pointed out that our surface has no defects, and the observed buckling is therefore not defect induced but is accomplished by a charge transfer within dimers.

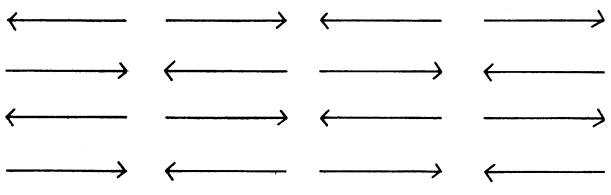

FIG. 1. The optimum structural configuration obtained by simulated annealing for the six-layer Si(001) slab sample. Each arrow represents a dimer, with the tip indicating the raised atom.

After having established its inherent asymmetric character, we will now consider the room-temperature behavior of dimers under the influence of a nearby defect. Since virtually all the experimentally observed defects appear in the form of individual missing dimers or small clusters of 2–3 missing dimers,[6] we shall investigate the behavior of dimers on a reconstructed Si(001) surface near a missing dimer vacancy (divacancy). In particular, we seek to examine whether such a defect could induce or stabilize the buckled configurations of neighboring dimers, and to understand how such interaction could induce the formation of ordered $p(2\times2)$ and $c(4\times2)$ regions in the vicinity.

To simulate the divacancy effects at room temperature, a dimer is removed from a reconstructed Si(001)-2×1 unbuckled surface, and the resulting "defective" surface is slowly heated to $T=300$ K. Figure 2(a) shows the atomic coordinates obtained by averaging over 4000 time steps (≈0.44 ps) during equilibration at room temperature, while Fig. 2(b) gives the corresponding dimer tilt for each dimer over the same interval. We observe that, in Fig. 2(b), buckling along the dimer row, in general, has no apparent decay in magnitude, but in directions other than $\langle\bar{1}10\rangle$ it decays slowly with distance from the defect. The relatively small buckling for dimer(9,12) and dimer(10,13) is due to their being pulled into the surface as a result of changes in local coordination at the defect site. In addition, they buckle in the same direction. Another interesting feature concerns the buckling directions of dimer(2,6) and dimer(16,20); their directions are such that the "raised" atoms are next to the defect.

The apparent nondecay in the $\langle\bar{1}10\rangle$ direction is most probably due to the small surface area of the simulation cell used, and this allows strain fields from adjacent diva-

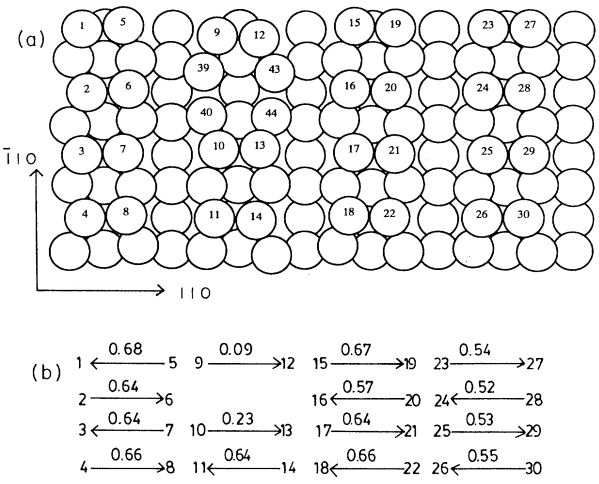

FIG. 2. The Si(001) surface at $T=300$ K. (a) Atomic coordinates averaged over 4000 time steps (≈0.44 ps). Four atomic layers are shown with atoms 39, 40, 43, and 44 being the exposed second-layer atoms. Numbers on each atom label the atomic indices. The missing dimer site is the divacancy. (b) Each arrow represents a dimer, with the tip indicating the raised atom. Real numbers on each arrow indicate the corresponding time-averaged tilt Δz (in Å) over the same time interval, while integer numbers label the atomic indices.

cancies to interact across the cell boundaries. This strong in-phase influence from these defects then leads to the observed slow decay along the row. We believe that the absence of symmetric dimers in Fig. 2(b) is due to the same reason. Clearly, it would be desirable to simulate defect properties with a larger surface unit cell, but the computational cost would be prohibitively expensive to make simulations of this scale practical and efficient. Nevertheless, the general trend that Δz [Fig. 2(b)] decreases with distance from the defect suggests symmetric dimers can exist at distances sufficiently far from the defect. This is verified by carrying out similar calculations for a reconstructed Si(001)-2×1 defect-free surface at room temperature. All dimers are observed to flip their buckling orientations alternately with time. The energy barrier between the two buckling configurations could now be overcome at room temperature such that on the time average, the dimers appear symmetric, a result that was reported earlier in MD simulations utilizing empirical interatomic potential functions.[11] This agrees well with STM observations that buckled dimers occur only in the vicinity of defects or step edges.[6,10] Hence our results provide strong theoretical support for the assertion that the defect induces dimer buckling.

As was noted earlier, dimer(9,12) and dimer(10,13), besides being twisted and pulled into the surface, are buckled in the same direction as well; in STM topographs, the "raised" atoms of these dimers would appear as very faint spots. We note further that the two second-layer dimers are slightly buckled and somewhat twisted [Fig. 2(a)]. This gives the divacancy an asymmetric character. Wolkow[10] has broadly divided the nature of defects into two categories: those that induce buckling and those that do not. He found that, in general, defects that induce breaking have an asymmetric character, while those that do not reveal no asymmetric structure. The defect studied in this work appears to belong to the former category. In addition, our results indicate that the electric charges located on the four atoms of the exposed second layer have an average value of about 3.83, 3.87, 3.80, and 3.90e for atoms 39, 40, 43, and 44 respectively, the "missing" charges being distributed to the surrounding atoms, particularly atoms 6 and 16.

We next examine the question of whether the defect could stabilize dimer buckling at room temperature, as speculated. We investigate this by considering whether the dimers at room temperature have sufficient thermal energy to enable them to flip in the opposite directions. This is done by calculating Δz in Fig. 3 as a function of time steps for several dimers. No buckled dimers are observed to flip their orientations in the opposite directions within the 4000 time steps [except for dimer(9,12) and dimer(10,13)] suggesting that the defect indeed has a strong stabilizing influence on them, restricting them to oscillate only about their pinned configurations.

STM images often reveal regions of $p(2\times2)$ and $c(4\times2)$ symmetries near defects and step edges, which are reproduced in this work. However, in recent years, a theoretical explanation for this occurrence has not been forthcoming. We therefore undertake in the next few paragraphs to provide a simple qualitative picture to explain the phase coexistence of $p(2\times2)$ and $c(4\times2)$ symmetries near the defect at room temperature. Consider an unbuckled Si(001)-2×1 reconstructed and defect-free surface at room temperature. As the surface dimer is removed to form a divacancy, the two dangling bonds associated with the removed dimer are eliminated and one new dangling bond on each of the four second-layer atoms 39, 40, 43, and 44 is produced [atomic indices are given in Fig. 2(a)]. Dimerization of these atoms in the direction parallel to the rows then eliminates these new dangling bonds.[15] In addition, they are also displaced into the surface to offset the sudden drop in the local coordination from the ideal value of 4. In the process the two adjacent dimers [dimer(9,12) and dimer(10,13)] of the same row are pulled into the surface [by about 0.4 Å, and 0.2 Å for dimer(9,12) and dimer(10,13), respectively] and toward the defect, resulting in a slight enlargement of the depression originally due to the divacancy. As the second-layer atoms form dimers with weak bonds between them, the elastic strain incurred is partially relieved when atoms 6 and 16 move out of the surface, producing the first buckled dimers with the "raised" atoms next to the defect [Fig. 2(b)] [Incidentally, it cannot be overemphasize that this feature (the raised atoms being adjacent to the defect) is responsible for the simultaneous formation of local $p(2\times2)$ and $c(4\times2)$ symmetries as will be seen below]. However, in doing so, this creates strain in the adjacent dimers of the same rows (rows A and C) and such strain is further reduced if these dimers buckle in the opposite directions with respect to dimer(2,6) and dimer(16,20), respectively. This dimer-dimer coupling via lattice strain finally causes rows A and C to buckle alternately from dimer to dimer [Fig. 4(a)].

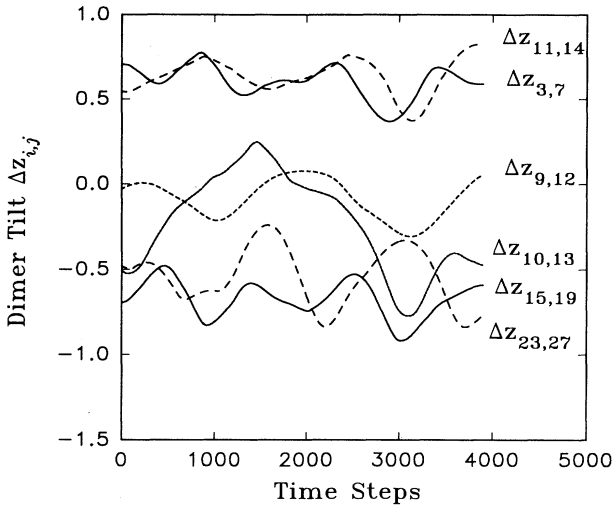

FIG. 3. The dimer tilt (in Å) as a function of time steps (one step corresponding to 1.1×10^{-16} s) calculated at $T=300$ K. $\Delta z_{i,j}$ is defined as the difference between the z coordinates (z_i-z_j) of atoms i and j with the z direction being normal to the surface. The atomic indices are given in Fig. 2(a).

Figure 4(a) depicts the important initial stage in the

formation of $p(2\times2)$ and $c(4\times2)$ regions. However, the exact details of these surface structural configurations would depend crucially on the structural properties of the second-layer dimers, dimer(39,40) and dimer(43,44). If these dimers buckle and twist in a way that makes dimer(9,12) and dimer(10,13) buckle in the same direction as is found in this work— and also exploiting the fact that the buckling direction always alternates from dimer to dimer—a reconstruction of the type given in Fig. 4(b) should result. In this schematic diagram, the surface cell is deliberately enlarged to contain more (imaginary) dimers, in the effort to emphasize clearly the formation regions of local $p(2\times2)$ and $c(4\times2)$ symmetries.

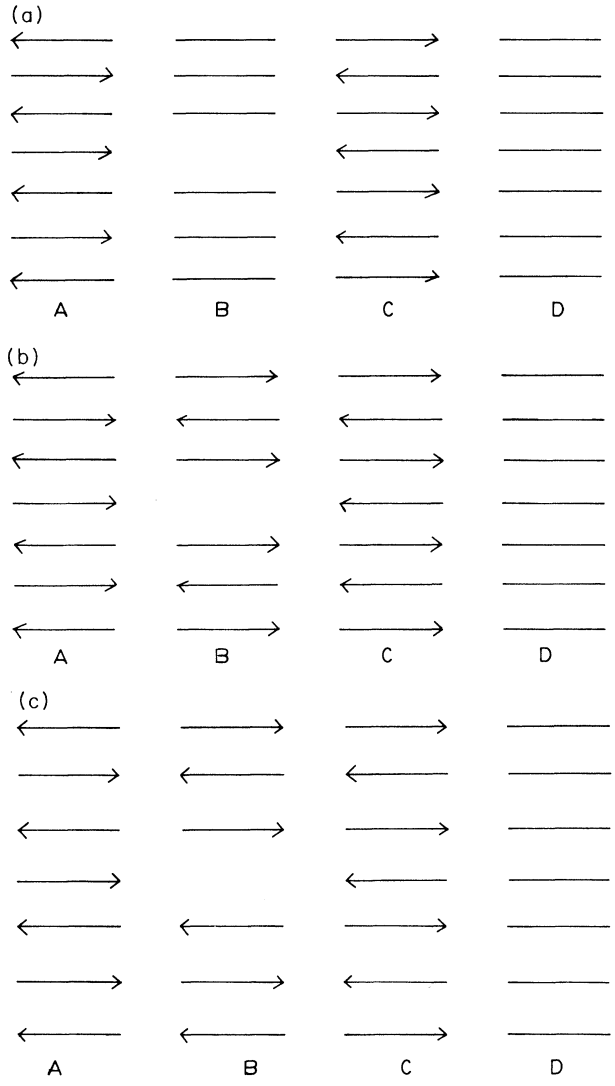

FIG. 4. Schematic diagrams showing stages of the various possible reconstructions (see text). (a) Buckling of dimer(2,6) and dimer(16,20) leads to the eventual alternate buckling in rows *A* and *C*. Horizontal bars represent symmetric dimers. (b) dimer(9,12) and dimer(10,13) buckle in the same direction, leading to the formation of regions with $p(2\times2)$ (from rows *B* and *C*) and $c(4\times2)$ (rows *A* and *B*) local symmetry. (c) $c(4\times2)\leftrightarrow p(2\times2)$ structural-phase transition, where the phase is interrupted at the divacancy.

However, a different and more interesting reconstruction pattern [Fig. 4(c)] could result if they behave otherwise to make dimer(9,12) and dimer(10,13) buckle opposite to each other. We see from rows *B* and *C* an interesting feature that exhibits a transition from a local $c(4\times2)$ symmetry at the bottom of the surface cell to a local $p(2\times2)$ symmetry at the top. A similar phase transition could also be seen in rows *A* and *B*. Incidentally, a structural phase transition of this type has been observed with STM.[6]

In either case, we note that the defect appears to induce the simultaneous formation of regions with $p(2\times2)$ and $c(4\times2)$ local symmetries. However, the formation of extended two-dimensional ordered structures is unclear and is possible due to the weak dipole-dipole interactions rather than via a lattice strain relief mechanism. As the dimer buckles, there is a charge transfer within the dimer and a dipole is created. This dipole then interacts with neighboring dimers of adjacent rows through electrostatic interactions to constitute perhaps the most important component in row-row coupling in the formation of extended two-dimensional domains of $p(2\times2)$- and $c(4\times2)$-like regions.

Finally, we wish to make some comments regarding the twisted dimer model first proposed by Yang, Jona, and Marcus.[16] They have managed to obtain good agreement between calculated and experimental low-energy electron diffraction (LEED) *I-V* data when dimers are assumed to be twisted so that their axes no longer lie in the $\langle 110\rangle$ direction. However, subsequent theoretical and experimental evidence does not appear to support this conclusion. In this work, we do not observe twisted dimers in our lowest-energy configuration; neither are they present in the defect-free surface at room temperature. However, in the presence of the defect, we observe significant twisting [Fig. 2(a)]. The twisting magnitudes decay rather rapidly with distance from the defect, so that for dimers more than about two dimers away they are practically untwisted. For instance, dimer(16,20) is twisted by 0.09 Å while dimer(25,29) is essentially untwisted. The pronounced twisting near the divacancy observed in Fig. 2(a) is perhaps due again to the small surface MD cell. However, the general trend should be reasonably unaffected. It should also be pointed out that the apparently untwisted dimers are observed to exhibit some sort of dynamical twisting, a behavior that is reminiscent of dimers exhibiting dynamical buckling on a defect-free surface at room temperature due to thermal excitations. Similar calculations for dimer twist Δy as a function of time yield results similar to Fig. 3.

IV. CONCLUSION

In conclusion, dimers are inherently asymmetric, but at sufficiently high temperatures and in the absence of defects, they oscillate so that on a time average they appear symmetric. However, in the presence of a divacancy, this defect not only induces nearby dimers to become buckled and twisted but it also pins them at their buckled

configurations since thermal excitations at room temperature are found to be insufficient to overcome the energy barrier for them to flip in the opposite directions. In addition, we note that both the buckling and twisting magnitudes decay with distance from the defect. We have also observed the formation of $c(4\times2)$- and $p(2\times2)$-like ordered regions in the vicinity of the defect, and the possible mechanisms leading to this phase coexistence have been discussed in detail.

ACKNOWLEDGMENTS

We wish to thank Dr. J. Q. Broughton and Dr. F. Ercolessi for their helpful advice in the course of our coding the program.

[1]Paul C. Weakliem and Emily A. Carter, J. Chem. Phys. **96**, 3240 (1992).

[2]D. J. Chadi, Phys. Rev. Lett. **43**, 43 (1979).

[3]J. H. Wilson, J. D. Todd, and A. P. Sutton, J. Phys. Condens. Matter **2**, 10259 (1990); M. T. Yin and M. L. Cohen, Phys. Rev. B **24**, 2303 (1981); C. K. Ong and B. C. Chan, J. Phys. Condens. Matter **1**, 3931 (1989).

[4]W. A. Harrison, Surf. Sci. **55**, 1 (1976).

[5]J. A. Appelbaum, G. A. Baraff, and D. R. Hamann, Phys. Rev. B **12**, 5749 (1975).

[6]R. M. Tromp, R. J. Hamers, and J. E. Demuth, Phys. Lett. **55**, 1303 (1985); R. J. Hamers, R. M. Tromp, and J. E. Demuth, Phys. Rev. B **34**, 5343 (1986).

[7]R. M. Tromp, R. G. Smeenk, F. W. Saris, and D. J. Chadi, Surf. Sci. **133**, 137 (1983).

[8]S. J. White and D. P. Woodruff, Surf. Sci. **64**, 131 (1977); S. Y. Tong and A. L. Moldonado, *ibid.* **78**, 459 (1978); J. J. Lander and J. Morrison, J. Chem. Phys. **37**, 729 (1962).

[9]M. J. Cardillo and G. E. Becker, Phys. Rev. Lett. **40**, 1148 (1978); Phys. Rev. B **21**, 1497 (1980).

[10]Robert A. Wolkow, Phys. Rev. Lett. **68**, 2636 (1992).

[11]P. C. Weakliem, G. W. Smith, and E. A. Carter, Surf. Sci. Lett. **232**, L219 (1990).

[12]F. S. Khan and J. Q. Broughton, Phys. Rev. B **39**, 3688 (1989).

[13]D. Tománek and M. A. Schlüter, Phys. Rev. Lett. **56**, 1055 (1986); Phys. Rev. B **36**, 1208 (1987); O. L. Alerhand and E. J. Mele, *ibid.* **35**, 5533 (1987).

[14]J. P. Rychaert, G. Ciccotti, and H. J. C. Berendsen, J. Comput. Phys. **23**, 327 (1977).

[15]K. C. Pandey, in *Proceedings of the Seventeenth International Conference on the Physics of Semiconductors,* edited by D. J. Chadi and W. A. Harrison (Springer-Verlag, New York, 1985).

[16]W. S. Yang, F. Jona, and P. M. Marcus, Phys. Rev. B **28**, 2049 (1983).